NUCLEAR THEORY, Vol. 41 (2024)
eds. M. Gaidarov, N. Minkov, Heron Press, Sofia

Superscaling Analysis of Inclusive Electron and Neutrino (Antineutrino) Scattering within the Coherent Density Fluctuation Model

M.V. Ivanov[1,2], **A.N. Antonov**[1]

[1]Institute for Nuclear Research and Nuclear Energy, Bulgarian Academy of Sciences, Tzarigradsko Shaussee 72, 1784 Sofia, Bulgaria
[2]South-West University "Neofit Rilski", 66 Ivan Mihaylov St., 2700 Blagoevgrad, Bulgaria

Abstract. The experimental data from quasielastic electron and (anti)neutrino scattering on ^{12}C are reanalyzed within a theoretical method in terms of a new scaling variable ψ^* suggested by the interacting relativistic Fermi gas model with scalar and vector interactions, which is known to generate a relativistic effective mass for the interacting nucleons. We construct a new scaling function $f^{\rm QE}(\psi^*)$ for the inclusive lepton scattering from nuclei within the coherent density fluctuation model (CDFM). The latter is a natural extension of the relativistic Fermi gas (RFG) model to finite nuclei. In this work, on the basis of the scaling function obtained within CDFM with a relativistic effective mass $m_N^* = 0.8m_N$, we calculate and compare the theoretical predictions with a large set of experimental data for inclusive (e, e') and (anti)neutrino cross sections. The model also includes the contribution of weak two-body currents in the two-particle two-hole sector, evaluated within a fully RFG. Good agreement with experimental data is found over the whole range of electron and (anti)neutrino energies.

1 Introduction

The superscaling phenomenon was firstly considered within the framework of the Relativistic Fermi Gas (RFG) model [1–6], where a properly defined function of the scaling ψ-variable was introduced. At large transferred momentum $q = |\mathbf{q}|$ ($q > 500$ MeV/c) the latter does not depend on q and the mass number. As pointed out in [4], however, the actual nuclear dynamical content of the superscaling is more complex than that provided by the RFG model. It was observed that the experimental data have a superscaling behavior in the low-ω side (ω being the transfer energy) of the quasielastic peak for large negative values of ψ (up to $\psi \approx -2$), while the predictions of the RFG model are $f(\psi) = 0$ for $\psi \leq -1$. This imposes the consideration of the superscaling in realistic finite systems. One of the approaches to do this was developed [7, 8] in the CDFM [9–16] which is related to the δ-function limit of the generator coordinate method [7, 17]. It was shown in [7, 8, 18] that the superscaling in nuclei

can be explained quantitatively on the basis of the similar behavior of the high-momentum components of the nucleon momentum distribution in light, medium and heavy nuclei. It is well known that the latter is related to the effects of the *NN* correlations in nuclei (see, *e.g.* [9, 10]).

In our previous works [7, 8, 18, 19] we obtained the CDFM scaling function $f(\psi)$ starting from the RFG model scaling function $f_{\rm RFG}(\psi)$ and convoluting it with the weight function $|F(x)|^2$ that is related equivalently to either the density $\rho(r)$ or the nucleon momentum distribution $n(k)$ in nuclei. Thus, the CDFM scaling function is an infinite superposition of weighted RFG scaling functions. This approach improves upon RFG and enables one to describe the scaling function for realistic finite nuclear systems. The CDFM scaling function has been used to predict cross sections for several processes such as the inclusive electron scattering in the QE and Δ- regions [19, 20] and neutrino (antineutrino) scattering both for charge-changing (CC) [20] and for neutral-current (NC) [21] processes. In our work [19] we reproduce experimental data of the inclusive electron scattering in the QE-region using CDFM scaling function which is obtained by the parameterizing the RFG scaling function and by the coefficient c_1, which helps us to account for the experimental fact of the asymmetry of the scaling function. The value of the coefficient c_1 ($c_1 \neq 3/4$) is taken in accordance with the empirical data (c_1 depends on the value of the momentum transfer in the QE peak).

In the present work we follow Ref. [22], where the ψ^* scaling idea is explored in the context of the Relativistic Mean Field (RMF) for nuclear matter. The new scaling function $f^*(\psi^*)$ including dynamical relativistic effects [22–25] is introduced through an effective mass into its definition. The resulting superscaling approach with relativistic effective mass (SuSAM*) model describes a large amount of the electron scattering data lying inside a phenomenological quasielastic band, and it has been extended recently successfully to the neutrino and antineutrino sector [26] giving a fair agreement with the data. An enhancement of the SuSAM* model is detailed in Refs. [27–30], where the responses of 2p2h meson exchange currents (MEC) are calculated consistently with the mean field model in nuclear matter. This is achieved by incorporating an effective mass and vector energy for the nucleon, thereby explicitly including the same medium modifications as the quasielastic responses. A systematic review of experimental data on quasielastic neutrino scattering reveals a reasonable agreement with the theoretical predictions derived from the extended SuSAM* model [30].

The SuSAM* model was first developed using the set of ^{12}C data [22, 23] and later applied to other nuclei in [24]. In Ref. [22] was obtained the best value of the effective mass $M^* = m_N^*/m_N = 0.8$, which we use in our present consideration. This value provides the best scaling behavior of the data with a large fraction of data concentrated around the universal scaling function of the relativistic Fermi gas

$$f_{\rm RFG}(\psi^*) = \frac{3}{4}(1-\psi^{*2})\theta(1-\psi^{*2}). \tag{1}$$

The ψ^* variable was inspired by the mean-field theory, that provides a reasonable description of the quasielastic response function [31, 32]. The important point is that in the interacting RFG model the vector and scalar potentials generate an effective mass m_N^* for the nucleon in the medium.

Our present approach, called CDFM$_{M^*}$ (CDFM with M^*), uses scaling function obtained within the CDFM model. It keeps the gauge invariance and describes the dynamical enhancement of both the lower components of the relativistic spinors and the transverse response function. In Ref. [33], we thoroughly examined the theoretical framework for deriving the CDFM$_{M^*}$ scaling function and the general formalism for characterizing the (e, e') and (anti)neutrino CC quasielastic double differential cross sections. In this study, we present our main results for the inclusive (e, e') and (anti)neutrino CC quasielastic cross sections using the CDFM$_{M^*}$ approach.

2 Results and Discussions

In this section we use the new scaling function of the CDFM$_{M^*}$ model (see Ref. [33]) to compute lepton scattering cross sections on ^{12}C. It is important to test CDFM$_{M^*}$ model for inclusive (e, e') scattering before to apply it to neutrino scattering. In Figure 1 we show the predictions of CDFM$_{M^*}$+MEC contribution (blue solid line) for the (e, e') cross section compared to the experimental data [37]. Also, the RFG$_{M^*}$+MEC results (green dashed line) are given. The contribution of meson exchange currents (MEC) is presented, separately. The evaluation of the 2p-2h pionic MEC contributions is performed within the RFG model in which a fully Lorentz covariant calculation of the MEC can be performed (see [38–40]). The CDFM$_{M^*}$ model description is quite acceptable using just one free parameter, namely the effective mass M^*, which is fixed to 0.8 in all performed calculations.

In Figures 2 and 3 we show the double differential cross section averaged over the neutrino and antineutrino energy flux against the kinetic energy of the final muon. The data are taken from the MiniBooNE Collaboration [34, 35]. We represent a large variety of kinematical situations where each panel refers to results averaged over a particular muon angular bin.

In this work we make use of the 2p-2h MEC model developed in Ref. [41], which is an extension to the weak sector of the seminal papers [38, 42, 43] for the electromagnetic case. The calculation is entirely based on the RFG model and it incorporates the explicit evaluation of the five response functions involved in inclusive neutrino scattering. We use a general parametrization of the MEC responses that significantly reduces the computational time. Its functional form for the cases of ^{12}C and ^{16}O is given in Refs. [44–46].

The results including both QE process (obtained within the CDFM$_{M^*}$ model) and 2p–2h MEC are compared with the data in Figures 2 and 3. The QE and 2p–2h MEC contributions are presented separately also in the figures. It should be noted the important role played by 2p-2h MEC to describe correctly the experi-

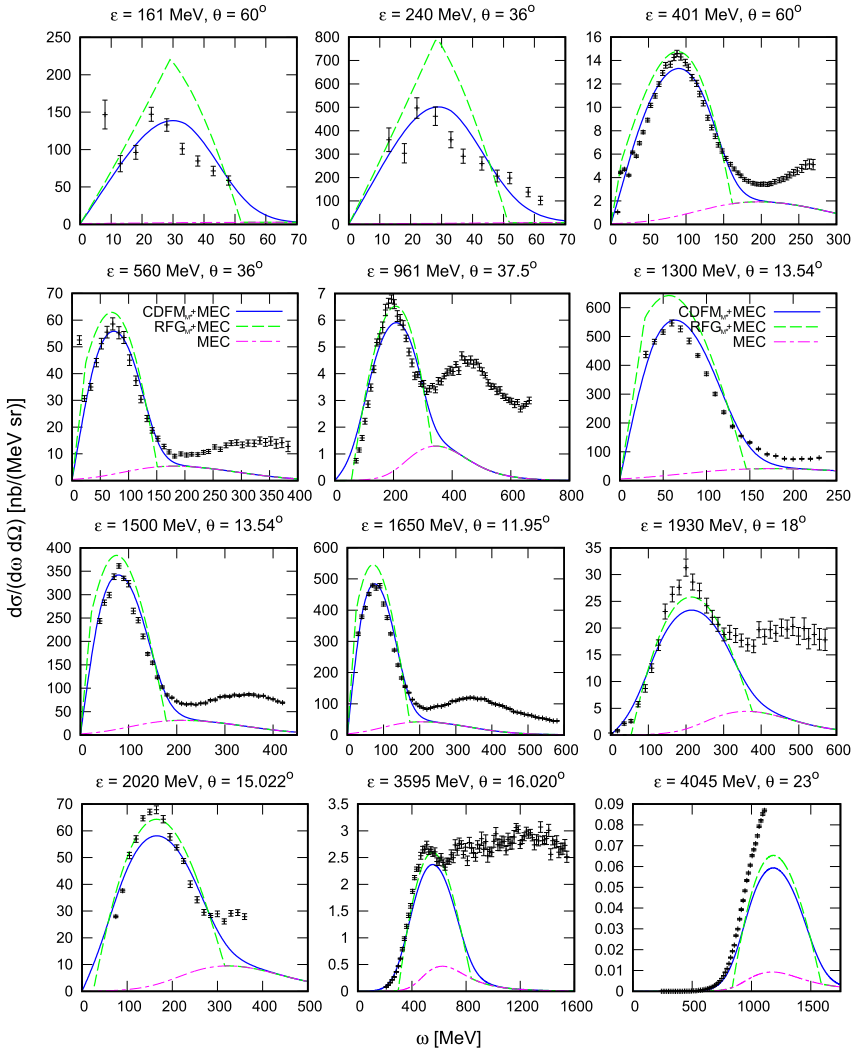

Figure 1. (Color online) The CDFM$_{M^*}$ results for the inclusive (e, e') cross section for several kinematics compared to the RFG$_{M^*}$ model and experimental data [37].

mental data of the order of ∼20–25% of the total response at the maximum. In the neutrino case (Figure 2) this relative strength is almost independent of the scattering angle. In the antineutrino case (Figure 3) the 2p-2h relative strength gets larger for backward scattering angles. This is due to the fact that the antineutrino cross section involves a destructive interference between the T and T' channels and is therefore more sensitive to nuclear effects.

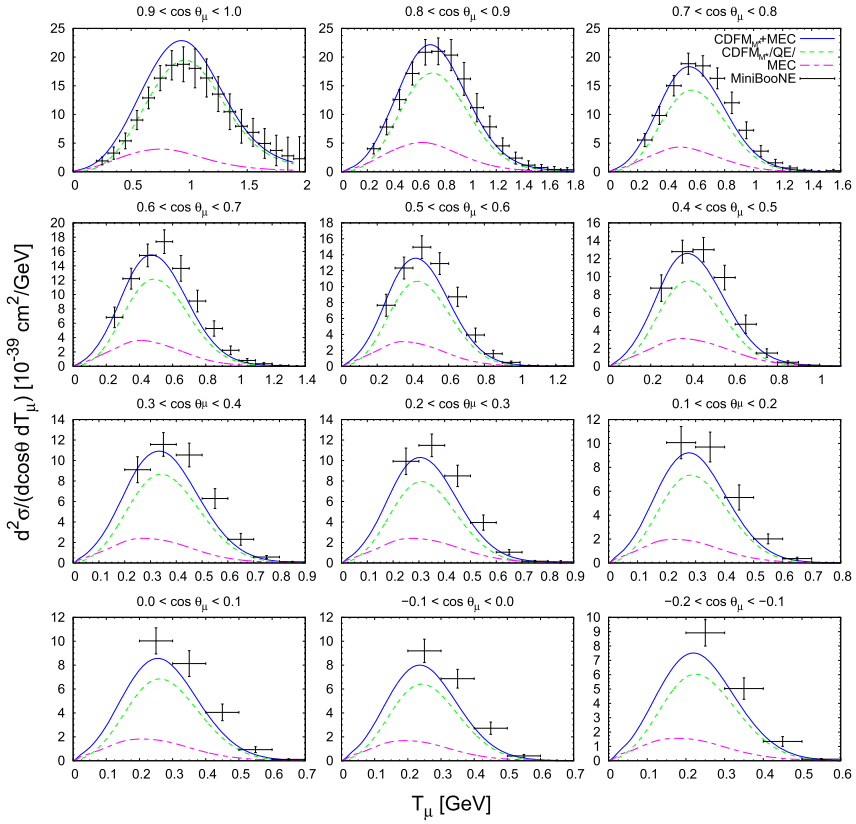

Figure 2. (Color online) MiniBooNE flux-folded double differential cross section per target neutron for the ν_μ CCQE process on ^{12}C displayed versus the μ^- kinetic energy T_μ for various bins of $\cos\theta_\mu$ obtained within the CDFM$_{M^*}$ model including MEC. 2p–2h MEC and QE (obtained within the CDFM$_{M^*}$ model) results are shown separately. The data are from [34].

Theoretical predictions within the CDFM$_{M^*}$ model including both QE and 2p-2h MEC contributions are in good agreement with the data in most of the kinematical situations explored. Only at scattering angles approaching 90° and above one can see a hint of a difference, although in these situations only a small number of data points with large uncertainties exist.

The CDFM$_{M^*}$ results for the total flux-unfolded integrated cross sections per nucleon are given in Figure 4 being compared with the MiniBooNE [34, 35] and NOMAD [36] data (up to 100 GeV). As can be seen in Figure 4, the 2p-2h MEC contributions are needed in order to reproduce the MiniBooNE data. Also, the contributions of different parts of the scaling to the total cross sections are presented in Figure 4. The main contribution to the cross sections comes

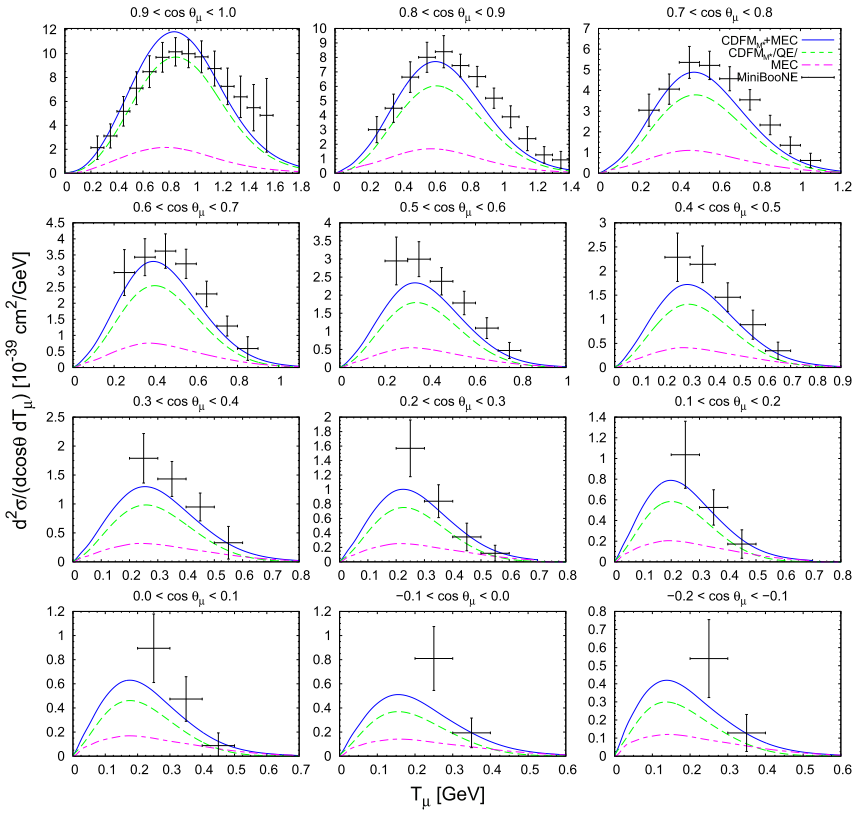

Figure 3. (Color online) As for Figure 2, but now for the $\overline{\nu}_\mu$ CCQE process on ^{12}C. The data are from [35].

from the part of the CDFM$_{M^*}$ scaling function between $-1 \leq \psi^* \leq 1$. The CDFM$_{M^*}$ model with 2p–2h MEC clearly overpredicts the NOMAD data. On the contrary, the results without MEC contributions (the pure QE results obtained within CDFM$_{M^*}$ model) are in good agreement with the NOMAD data. This result is consistent with the setup of the NOMAD experiment that, unlike MiniBooNE, can select true QE, rather than the "QE-like" events. The role of the 2p-2h MEC is very important at all neutrino energies, getting an almost constant value of the order of $\sim 30\% - 35\%$ compared with the pure QE contribution. Here, we would like to mention that the quasielastic data themselves have been measured not directly but have been deduced from the so-called quasielastic-like data by subtracting a background of events in which pions are firstly produced, but then reabsorbed again. This background was determined from the calculations with an event generator. Thus, the final QE + 2p-2h data invariably contain some model dependence [47].

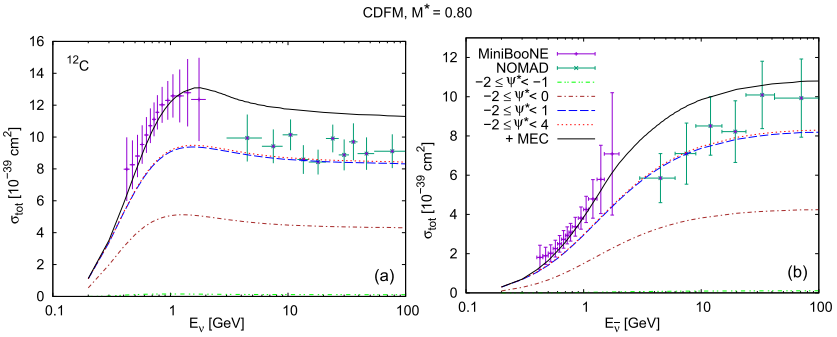

Figure 4. (Color online) CCQE ν_μ–^{12}C ($\overline{\nu}_\mu$–^{12}C) total cross section per neutron (proton) as a function of the neutrino energy. The left panel (a) corresponds to neutrino cross sections and the right one (b) to antineutrino reactions. The data are from MiniBooNE [34, 35] and NOMAD [36] experiments.

3 Conclusions

It is shown in our work that the CDFM$_{M^*}$ model describes successfully inclusive (e, e') and $\nu(\overline{\nu})$ CCQE quasielastic cross section on the basis of the new scaling variable ψ^*, of the empirical density distribution of protons to determine the weight function $|F(x)|^2$, and of the corresponding scaling function $f^{\rm QE}(\psi^*)$. We note that in the CDFM$_{M^*}$ model an effective mass $M^* = m_N^*/m_N = 0.8$ is used. The latter is originating from the interacting RFG model in which the vector and scalar potentials generate the effective mass of the nucleon in medium. We should emphasize that the CDFM$_{M^*}$ scaling function keeps the gauge invariance (that is not the case in the SuSA approach) and describes the dynamical enhancement of the lower components of the relativistic spinors, as well as the transverse response function. In addition, we note the important fact that in the CDFM$_{M^*}$ model the weight and scaling functions are normalized to unity. It is pointed out that the constructed realistic CDFM$_{M^*}$ scaling function is an essential ingredient in this approach for the description of the processes of lepton scattering from nuclei.

It is important to recognize that the parametrization of the 2p2h MEC used in this analysis originates from the RFG model with an effective mass of $M^* = 1$. An alternative parametrization for electroweak 2p2h MEC responses, computed in the RMF with an effective mass of $M^* = 0.8$, has been proposed in recent studies [27, 28]. This new parametrization, utilizing a semiempirical formula, may offer advantages over the CDFM$_{M^*}$ model. Thus, the first step to improve our model is to implement this alternative parametrization to assess its impact on future research. Additionally, a prospective project could involve expanding the scaling method by applying a realistic CDFM$_{M^*}$ scaling function to predict outcomes for charge-changing neutrino and antineutrino scattering from nuclei in the Δ-region.

References

[1] W.M. Alberico, A. Molinari, T.W. Donnelly, E.L. Kronenberg, J.W. Van Orden, *Phys. Rev. C* **38** (1988) 1801-1810.

[2] M. Barbaro, R. Cenni, A.D. Pace, T. Donnelly, A. Molinari, *Nucl. Phys. A* **643** (1998) 137-160.

[3] T.W. Donnelly, I. Sick, *Phys. Rev. Lett.* **82** (1999) 3212-3215.

[4] T.W. Donnelly, I. Sick, *Phys. Rev. C* **60** (1999) 065502.

[5] C. Maieron, T.W. Donnelly, I. Sick, *Phys. Rev. C* **65** (2002) 025502.

[6] M.B. Barbaro, J.A. Caballero, T.W. Donnelly, C. Maieron, *Phys. Rev. C* **69** (2004) 035502.

[7] A.N. Antonov, M.K. Gaidarov, D.N. Kadrev, M.V. Ivanov, E. Moya de Guerra, J.M. Udias, *Phys. Rev. C* **69** (2004) 044321.

[8] A.N. Antonov, M.K. Gaidarov, M.V. Ivanov, D.N. Kadrev, E. Moya de Guerra, P. Sarriguren, J.M. Udias, *Phys. Rev. C* **71** (2005) 014317.

[9] A.N. Antonov, P.E. Hodgson, I.Z. Petkov, "*Nucleon Momentum and Density Distributions in Nuclei*". Clarendon Press, Oxford, 1988.

[10] A.N. Antonov, P.E. Hodgson, I.Z. Petkov, "*Nucleon Correlations in Nuclei*". Springer-Verlag, Berlin-Heidelberg-New York, 1993.

[11] A.N. Antonov, V.A. Nikolaev, I.Z. Petkov, *Bulg. J. Phys.* **6** (1979) 151-158.

[12] A.N. Antonov, V.A. Nikolaev, I.Z. Petkov, *Z. Phys. A* **297** (1980) 257-260.

[13] A.N. Antonov, V.A. Nikolaev, I.Z. Petkov, *Z. Phys. A* **304** (1982) 239-243.

[14] A.N. Antonov, V.A. Nikolaev, I.Z. Petkov, *Il Nuovo Cimento A* **86** (1985) 23-31.

[15] A.N. Antonov, E.N. Nikolov, I.Z. Petkov, C.V. Christov, P.E. Hodgson, *Il Nuovo Cimento A* **102** (1989) 1701-1715.

[16] A.N. Antonov, D.N. Kadrev, P.E. Hodgson, *Phys. Rev. C* **50** (1994) 164-167.

[17] J.J. Griffin, J.A. Wheeler, *Phys. Rev.* **108** (1957) 311-327.

[18] A.N. Antonov, M.V. Ivanov, M.K. Gaidarov, E. Moya de Guerra, P. Sarriguren, J.M. Udias, *Phys. Rev. C* **73** (2006) 047302.

[19] A.N. Antonov, M.V. Ivanov, M.K. Gaidarov, E. Moya de Guerra, J.A. Caballero, M.B. Barbaro, J.M. Udias, P. Sarriguren, *Phys. Rev. C* **74** (2006) 054603.

[20] M.V. Ivanov, M.B. Barbaro, J.A. Caballero, A.N. Antonov, E. Moya de Guerra, M.K. Gaidarov, *Phys. Rev. C* **77** (2008) 034612.

[21] A.N. Antonov, M.V. Ivanov, M.B. Barbaro, J.A. Caballero, E. Moya de Guerra, M.K. Gaidarov, *Phys. Rev. C* **75** (2007) 064617.

[22] J.E. Amaro, E. Ruiz Arriola, I. Ruiz Simo, *Phys. Rev. C* **92** (2015) 054607.

[23] J.E. Amaro, E. Ruiz Arriola, I. Ruiz Simo, *Phys. Rev. D* **95** (2017) 076009.

[24] V.L. Martinez-Consentino, I. Ruiz Simo, J.E. Amaro, E. Ruiz Arriola, *Phys. Rev. C* **96** (2017) 064612.

[25] J.E. Amaro, V.L. Martinez-Consentino, E. Ruiz Arriola, I. Ruiz Simo, *Phys. Rev. C* **98** (2018) 024627.

[26] I. Ruiz Simo, V.L. Martinez-Consentino, J.E. Amaro, E. Ruiz Arriola, *Phys. Rev. D* **97** (2018) 116006.

[27] V.L. Martinez-Consentino, I. Ruiz Simo, J.E. Amaro, *Phys. Rev. C* **104** (2021) 025501.

[28] V.L. Martinez-Consentino, J.E. Amaro, I. Ruiz Simo, *Phys. Rev. D* **104** (2021) 113006.

[29] V.L. Martinez-Consentino, J.E. Amaro, P.R. Casale, I. Ruiz Simo, *Phys. Rev. D* **108** (2023) 013007.

[30] V.L. Martinez-Consentino, J.E. Amaro, *Phys. Rev. D* **108** (2023) 113006.

[31] R. Rosenfelder, *Ann. Phys.* **128** (1980) 188-240.

[32] B.D. Serot, J.D. Walecka, "*Relativistic Nuclear Many-Body Theory*", pp. 49-92. Springer US, Boston, MA, 1992.

[33] M.V. Ivanov, A.N. Antonov, *Phys. Rev. C* **109** (2024) 064621.

[34] A. Aguilar-Arevalo, et al., (MiniBooNE Collaboration), *Phys. Rev. D* **81** (2010) 092005.

[35] A.A. Aguilar-Arevalo, et al., (MiniBooNE Collaboration), *Phys. Rev. D* **88** (2013) 032001.

[36] V. Lyubushkin, et al., (NOMAD Collaboration), *Eur. Phys. J. C* **63** (2009) 355-381.

[37] O. Benhar, D. Day, I. Sick, *Rev. Mod. Phys.* **80** (2008) 189-224; https://discovery.phys.virginia.edu/research/groups/qes-archive/.

[38] A. De Pace, M. Nardi, W. Alberico, T. Donnelly, A. Molinari, *Nucl. Phys. A* **726** (2003) 303-326.

[39] I.R. Simo, C. Albertus, J.E. Amaro, M.B. Barbaro, J.A. Caballero, T.W. Donnelly, *Phys. Rev. D* **90** (2014) 033012.

[40] G.D. Megias, T.W. Donnelly, O. Moreno, C.F. Williamson, J.A. Caballero, R. González-Jiménez, A. De Pace, M.B. Barbaro, W.M. Alberico, M. Nardi, J.E. Amaro, *Phys. Rev. D* **91** (2015) 073004.

[41] I. Ruiz Simo, J.E. Amaro, M.B. Barbaro, A. De Pace, J.A. Caballero, T.W. Donnelly, *J. Phys. G* **44** (2017) 065105.

[42] J.W. Van Orden, T.W. Donnelly, *Annals Phys.* **131** (1981) 451–493.

[43] J.E. Amaro, C. Maieron, M.B. Barbaro, J.A. Caballero, T.W. Donnelly, *Phys. Rev. C* **82** (2010) 044601.

[44] G.D. Megias, J.E. Amaro, M.B. Barbaro, J.A. Caballero, T.W. Donnelly, I.R. Simo, *Phys. Rev. D* **94** (2016) 093004.

[45] G.D. Megias, J.E. Amaro, M.B. Barbaro, J.A. Caballero, T.W. Donnelly, *Phys. Rev. D* **94** (2016) 013012.

[46] G.D. Megias, M.B. Barbaro, J.A. Caballero, J.E. Amaro, T.W. Donnelly, I.R. Simo, J. W. V. Orden, *J. Phys. G: Nucl. Part. Phys.* **46** (2018) 015104.

[47] O. Lalakulich, U. Mosel, *Phys. Rev. C* **87** (2013) 014602.